High mobility p-type tin oxide thin-film by adopting passivation layer

Song-Yi Ahn[1], Hyun-Suk Kim

[1]Advanced Nanomaterials and Device Laboratory, Department of Materials Science and Engineering, Chungnam National University, 99 Daehak-ro, Yuseong-gu, Daejeon 305-764
Keywords: p-type SnO, thin-film transistors, SiO_2 passivation

ABSTRACT

The effects of SiO_2 passivation on tin monoxide (SnO) semiconductor was investigated. In X-ray photoelectron spectroscopy studies revealed that the tail-state above valence band maximum was clearly detected in SiO_2-capped SnO film which may improve the p-type conductivity. As a result, the resulting SnO thin-film transistors show enhanced electrical properties.

1 INTRODUCTION

Recently, thin-film transistors (TFTs) based on metal oxide semiconductors such as In-Ga-Zn-O (IGZO) have attracted considerable attention for pixel switching devices in flat-panel displays owing to their relatively high performance and stability compared to amorphous silicon [1,2]. Commercial products incorporating TFT backplanes based on n-type IGZO are already available in the market. However, p-type oxide semiconductors do not yet have sufficient electrical properties and require further study [3]. To date, the most promising candidates for the channel materials for p-type oxide TFTs are copper oxide (Cu_xO), nickel oxide (NiO_x) and tin monoxide (SnO) [3]. Among them, SnO has attracted considerable attention as a channel material for p-type oxide TFTs due to high hole motilities. In SnO, Sn 5s and O 2p orbitals are located at almost the same energy level near the valence band maximum (VBM) by hybridization. Such a configuration forms less-localized VBM states, creating relatively fast pathways for hole carriers. P-type conductivity of SnO_x is mainly attributed to Sn vacancies and oxygen interstitials [4]. The metastable SnO phase is transformed into SnO_2 phase in the air atmosphere, and p-type characteristics are degradation. So the passivation layer is required. Previous studies have reported the use of Al_2O_3 and PMMA passivation for SnO TFTs [2]. This work shows that SnO TFTs with SiO_2 passivation layer has high field effect mobility.

2 EXPERIMENT

SnO thin films were deposited by reactive radio frequency magnetron sputtering with 3-inch diameter metal Sn target. The applied RF power and gas mixing ratio of Ar/O_2 were fixed at 50 W and 5/0.5 (sccm), respectively. The microstructures of SnO and SiO_2/SnO thin films were analyzed by grazing incidence angle X-ray diffraction (GIAXRD) using a Cu kα radiation [D8 DISCOVER, Bruker AXS]. The surface morphologies were studied by atomic force microscopy (AFM). The chemical bonding states of nitrogen and oxygen components were examined by X-ray photoelectron spectroscopy (XPS) using a monochromatic Mg Kα (1253.6 eV) source and a pass energy of 50 eV. The optical transmittance and bandgap values were extracted using a Transmittance UV-vis Spectrometer (S-3100, SCINCO) in the range of 200-1000 nm. Hall measurements were also carried out to observe the electrical characteristics of thin films. (HMS-5500, ECOPIA). SnO TFTs with bottom gate structure were fabricated on highly doped p-type Si substrate with thermally grown 100 nm thick SiO_2 gate dielectrics. After depositing the tin oxide active layer, post-annealing was conducted at 300 ℃ for 1 hours in air atmosphere by rapid thermal annealing system (RTA). The source-drain electrodes consist of an Ni film with 100 nm fabricated by thermal evaporation. Both the semiconductor and the source-drain electrodes were patterned by shadow mask with a width and length of 800 and 200 μm, respectively.

To study the effect of passivation, SiO_2 was deposited under the condition of 50 W RF power and mixing ratio of Ar/O_2 = 10/5 (sccm). The thickness of the SiO_2 passivation layer was 10 nm, and annealed at 300 ℃ in air for 30 min by the hot plate. Fig. 1 depicts a cross-sectional schematic diagram of the final device structure. The transfer properties were analyzed using an HP 4156B semiconductor parameter analyzer in the dark under ambient conditions.

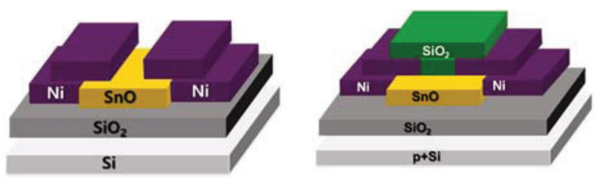

Fig. 1. schematic cross-section of p-type SnO TFTs (a) without SiO_2 passivation and (b) with SiO_2 passivation

3 RESULTS & DISCUSSION

Fig.2 consists of the XRD patterns for SiO_2/SnO thin film. (101) and (110) planes of SnO are observed, consistent with the tetragonal structure. Fig.3 shows the surface morphologies of the SnO and SiO_2/SnO thin films analyzed by AFM. In SnO thin film, the root-mean-square (RMS) surface roughness is 0.14 nm, while SiO_2 with 10 nm thickness in SnO thin films (SiO_2/SnO) exhibit slightly rough surface with RMS roughness of 0.42 nm.

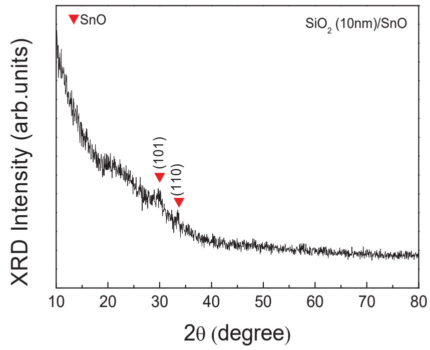

Fig. 2. XRD patterns of SiO_2 /SnO thin films

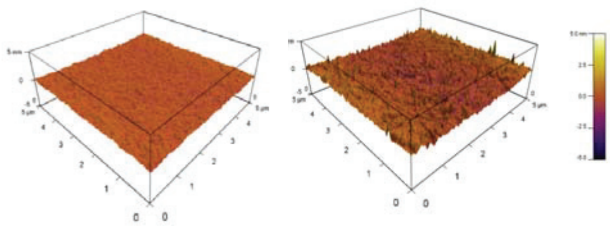

(a) SnO
RMS: 0.14 nm

(b) SiO_2/SnO
RMS: 0.42 nm

Fig. 3. Atomic force microscope images of films: (a) SnO on SiO_2 substrate and (b) SiO_2/SnO on SiO_2 substrate

Fig. 4(a) shows the optical transmittance of as-deposited SnO, annealed SnO and SiO_2 /SnO thin films measured in the wavelength range between 200 and 1000 nm. Figure 4 (b) shows how Tauc's law is used to extract optical bandgap values of 1.56 eV, 2.71 eV and 3.19 eV for deposited SnO, annealed SnO and SiO_2 / SnO thin films, respectively. (Theoretical value of SnO is 2.7 eV [6]). Fig. 4(c) shows the absorption coefficient spectra as a function of photon energy of the as-deposited and annealed SnO thin films. The tail state extending in the bandgap is called the Urbach tail and its slope reflects the number of localized trap states. The small slope of the Urbach tail suggests that it has a large amount of localized trap state in the optical bandgap [7]. As the absorption spectra of pristine and annealed films in the subgap region show that annealed SnO exhibits smaller subgap defect absorption than as-deposited SnO thin film (i.e., region of the blue circle marked with E_g < 2.71 eV). In the case of annealed SnO thin film, it suggests the high mobility.

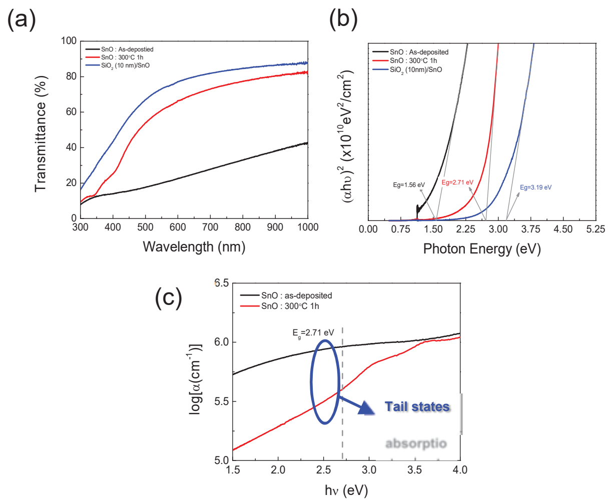

Table 1. summarizes the electrical parameters obtained by Hall effect measurements, which show that the hall concentration decreases from 5.65 x 10^{20} /cm^3

Fig. 4. (a) Transmittance spectra of SnO and SiO_2/SnO thin films. (b) Optical bandgap with SnO and SiO_2/SnO layer using Tauc's plot. (c) The tail state absorption with respect to SnO thin films.

to 9.76 x 10^{17} /cm^3, but the mobility increases from 0.47 cm^2/Vs to 3.99 cm^2/Vs.

	Carrier concentration (/cm^3)	Mobility (cm^2/Vs)
As-deposited	5.65 x 10^{20}	0.47
300℃ 1h (air)	9.76 x 10^{17}	3.99

Table 1. Hall measurement results of as-deposited SnO and annealed SnO thin films.

Fig. 5 shows the valence band profile near the valence band maximum of SnO and SiO_2/SnO thin films analyzed by XPS. The valence band maximums of the SnO and SiO_2/SnO film were located at 1.4 eV and 1.3 eV from the valence band edge. The slightly large tail state (i.e., region of the green circle marked) near valence band maximum of SiO_2/SnO thin films would act as acceptor to improve p-type conductivity. The relative atomic compositions of SnO and SiO_2/SnO thin films obtained by XPS depth profiling are listed in Table 2. SnO film is O-rich conditions, whereas SiO_2/SnO film is Sn-rich conditions. At that point, it was found that the passivation layer perfectly promotes SnO formation.

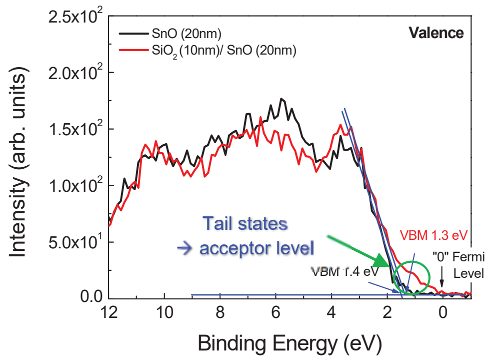

Fig. 5. Valence band spectra of SnO and SiO_2/SnO channel and interfacial layers analyzed by XPS.

(a)

	C	O	Si	Sn
500V 10s	3.0	53.0	-	44.0
1kV 10s	-	51.3	-	48.7

(b)

	C	O	Si	Sn
500V 10s	2.9	65.9	30.8	0.4
1kV 50s	1.5	67.1	28.3	3.1
1kV 80s	1.3	60.7	21.8	16.2
1kV 110s	-	48.8	8.0	43.2
1kV 160s	-	43.5	-	56.5
1kV 180s	-	42.2	-	57.8

Table 2. The atomic compositions of (a) SnO thin film and (b) SiO_2/SnO film obtained by XPS analysis

Fig. 6 depicts the electrical characteristics of SnO TFTs with and without SiO_2 passivation layer. Fig. 6(a) shows the transfer curve of the fabricated SnO TFTs with and without SiO_2 passivation layer measured at V_{DS} of -10 V and the V_{GS} range of -30 to 30 V. All TFTs exhibit a p-type transistor behavior. In SnO TFTs without passivation, on-off current ratio and field effect mobility is 5.8 and 1.25 x 10^{-4} cm^2/Vs, respectively. whereas, SnO TFTs with passivation layer observed on-off ratio and field effect mobility of 3.95 x 10^2 and 1.56 cm^2/Vs, respectively. Table 3. shows a comparison with various passivation. The output curve properties of the SnO TFT before and after deposit the passivation layer are shown in Fig. 6(b). SnO TFT with passivation layer exhibits clear pinch-off and current saturation without current crowding compared to SnO TFT without passivation layer. Overall, SnO TFT with passivation layer shows improved p-type electrical properties.

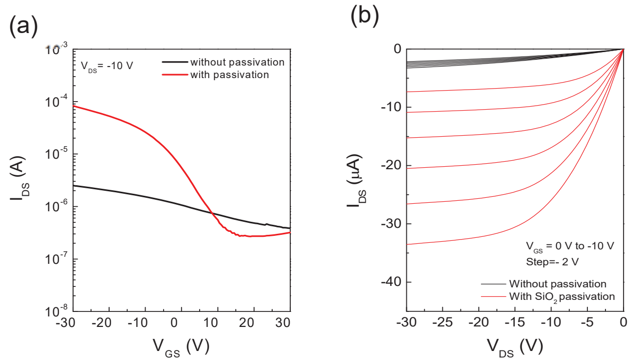

Fig. 6. (a) Transfer curves of the SnO TFT before and after using the passivation layer. (b) Output curves of SnO TFTs without and with SiO_2 passivation layer.

Passivation	Field effect mobility (cm^2/Vs)
With SiO_2	1.56
With Al_2O_3 [2]	0.16
With PMMA [2]	0.24

Table 3. Comparison of characteristics of various passivation

4 CONCLUSIONS

In the present work, the properties of SnO thin films with and without SiO_2 passivation layer and the related TFTs were investigated. Chemical analysis indicates that states above the valence band maximum were detected in SiO_2 passivated SnO, which would be acceptor level in the shallow states and tail states. Also, XPS depth analysis shows that SiO_2 passivation layer promotes p-type SnO formation. In addition, the SnO TFTs without SiO_2 passivation layer exhibited $I_{on/off}$ ratio of 6.50 and field effect mobility of 0.01 cm^2/Vs, respectively. After adopting passivation of SnO TFTs, $I_{on/off}$ ratio of 3.10x10^2 and field effect mobility of 1.16 cm^2/Vs were observed. In summary, the SiO_2 passivation layer by sputtering is effective method to improve the electrical characteristics of SnO TFT.

5 Reference

[1] Ogo, Y.; Hiramatsu, H.; Nomura, K.; Yanagi, H.; Kamiya, T.; Hirano, M.; Hosono, H. “p-channel thin-

films transistor using p-type oxide semiconductor, SnO" Appl. Phys. Lett., Vol. 93, issue 3, pp. 032113 (2008)

[2] Qu, Y.; Yang, J.; Li, Y.; Zhang, J.; Wang, Q.; Song, A.; Xin, Q. "Organic and inorganic passivation of p-type SnO thin-film transistors with different active layer thicknesses" Semicond. Sci. Technol., Vol. 33, No. 7, pp. 075001 (2018)

[3] Hsu, P.; Chen, W.; Tsai, Y.; Kung, Y.; Chang, C.; Hsu, C.; Wu, C.; Hsieh, H. "Fabrication of p-Type SnO Thin-Film Transistors by Sputtering with Practical Metal Electrodes" Jpn. J. Appl. Phys., Vol. 52, No. 52, pp. 05DC07 (2013)

[4] Bae, S.; Kwon, S.; Jeong, H.; Kwon, H. "Demonstration of high-performance p-type tin oxide thin-film transistors using argon-plasma surface treatments" Semicond. Sci. Technol., Vol. 32, No. 7, pp. 075006 (2017)

[5] Fortunato, E.; Barros, R.; Barquinha, P.; Figueiredo, V.; Park, A.; Hwang, C.; Martins, R. "Transparent p-type SnO_x thin film transistors produced by reactive rf magnetron sputtering followed by low temperature annealing" Appl. Phys. Lett., Vol. 97, issue 5, pp. 052105 (2010)

[6] Hong, S.; Park, S.P.; Kim, Y.; Kang, B.H.; Na, J.W.; Kim, H.J. "Low-temperature fabrication of an HfO_2 passivation layer for amorphous indium-gallium-zinc oxide thin film transistors using a solution process" *Sci Rep*. Vol. 7, issue 1, pp. 16265 (2017)

[7] Lee, J.H.; Choi, Y.; Jeong, C.Y.; Jung, D.K. "Electrical Instability of p-Channel SnO Thin-Film Transistors Under Light Illumination" Electron Device Lett., Vol. 37, No. 3, pp. 295-298

[8] Shijeesh, M.R.; Jayaraj. M.K. "Low temperature fabrication of CuxO thin-film transistors and investigation on the origin of low field effect mobility" J. Appl. Phys., Vol. 123, No. 16, pp. 161538